


Article

Design, Synthesis and Bioactive Evaluation of Oxime Derivatives of Dehydrocholic Acid as Anti-Hepatitis B Virus Agents

Zhuocai Wei ^{1,†}, Jie Tan ^{1,2,†}, Xinhua Cui ¹, Min Zhou ¹, Yunhou Huang ¹, Ning Zang ³, Zhaoni Chen ⁴ and Wanxing Wei ^{1,*} 

¹ College of Chemistry and Chemical Engineering, Guangxi University, Nanning 530004, China; liveupto123@163.com (Z.W.); yulitanjie@163.com (J.T.); cuixinhua123@163.com (X.C.); leelmm@gxu.edu.cn (M.Z.); 1814302009@st.gxu.edu.cn (Y.H.)

² Nanning Center for Disease Control and Prevention, Nanning 530028, China

³ School of Basic Medical Science, Guangxi Medical University, Nanning 530021, China; zangninggxnn@163.com

⁴ Pharmaceutical College, Guangxi Medical University, Nanning 530021, China; wonderyao@163.com

* Correspondence: wxwei@gxu.edu.cn

† These authors contributed equally to this work.

Received: 5 June 2020; Accepted: 17 July 2020; Published: 24 July 2020



Abstract: Oxime derivatives of dehydrocholic acid and its esters were designed for anti-hepatitis B virus (HBV) drugs according to principles of assembling active chemical fragments. Twelve compounds were synthesized from dehydrocholic acid by esterification and oxime formation, and their anti-hepatitis B virus (HBV) activities were evaluated with HepG 2.2.15 cells. Results showed that 5 compounds exhibited more effective inhibition of HBeAg than positive control, among them **2b-3** and **2b-1** showed significant anti-HBV activities on inhibiting secretion of HBeAg ($IC_{50} (2b-3) = 49.39 \pm 12.78 \mu\text{M}$, $SI_{(2b-3)} = 11.03$; $IC_{50} (2b-1) = 96.64 \pm 28.99 \mu\text{M}$, $SI_{(2b-1)} = 10.35$) compared to the Entecavir ($IC_{50} = 161.24 \mu\text{M}$, $SI = 3.72$). Molecular docking studies showed that most of these compounds interacted with protein residues of heparan sulfate proteoglycan (HSPG) in host hepatocyte and bile acid receptor.

Keywords: dehydrocholic acid; oxime derivatives; anti-HBV; designation; synthesis

1. Introduction

Hepatitis B is a potentially life-threatening liver infection caused by the hepatitis B virus (HBV), and still a major global health problem, which causes chronic infection, and puts people at a high risk of death from cirrhosis and liver cancer [1,2]. According to World Health Organization (WHO) reports, an estimated 257 million people are living with the hepatitis B virus infection in the world (defined as hepatitis B surface antigen positive). In 2015, hepatitis B resulted in 887,000 deaths, mostly from complications (including cirrhosis and hepatocellular carcinoma) [3]. The nucleos(t)ide analogues are recommended for the treatment of chronic hepatitis B in the current consensus guidelines due to their significant suppression of HBV replication [4–7]. Unfortunately, this treatment is not satisfactory due to the limitations and side effects of nucleos(t)ide drugs. HBV therapy with nucleoside analogs, in long term, has developed resistance and obvious decreased inhibition effects [8–10]. The disadvantages of nucleoside analogs prompted us and other researchers to invent and find new structural non-nucleoside analog compounds [11–16]. Many anti-HBV bioactive non-nucleoside analog compounds have been designed and developed on the basis of their interactions with receptor using molecular docking [17–21]. When HBV receptor binding domain PreS1 and PreS2 protein (including L protein, M protein and

S protein) interact with small molecules, the virus will not allow entry to hepatocyte. A receptor, heparan sulfate proteoglycan (HSPG), which is critical for virus attachment and helps enrich virions on the cell surface (bringing them in close proximity to the receptor) from pre-S2 in hepatocyte interacts with small molecules; the virus will be inhibited to attach the hepatocyte and endocytosis will not be allowed [22]. Cholic acids and their derivatives were reported as liver-targeted vehicles for drug delivery due to their existence in the liver with no side effects and metabolization through enterohepatic circulation [23–26]. Dehydrocholic acid (DHCA) is a derivative of cholic acid [27] containing one carboxyl group and three carbonyl groups. Drugs targeted and concentrated to the liver organ will increase their anti-HBV effectivity and decrease side effects. Therefore DHCA, with reactive functional groups, was considered as a liver-target vehicle to deliver drugs to the liver in our present work. Based on the bioactivities of DHCA and oximes in our previous works [28–30], the introduction of the oxime group to DHCA should be suggested to possess liver-targeted and anti-HBV activities. So, a series of oxime derivatives of DHCA were designed, synthesized, and screened for anti-HBV activity *in vitro* in this work, and molecular docking studies were carried out to investigate the relationship of structure and bioactivity of these compounds using a molecular operating environment (MOE).

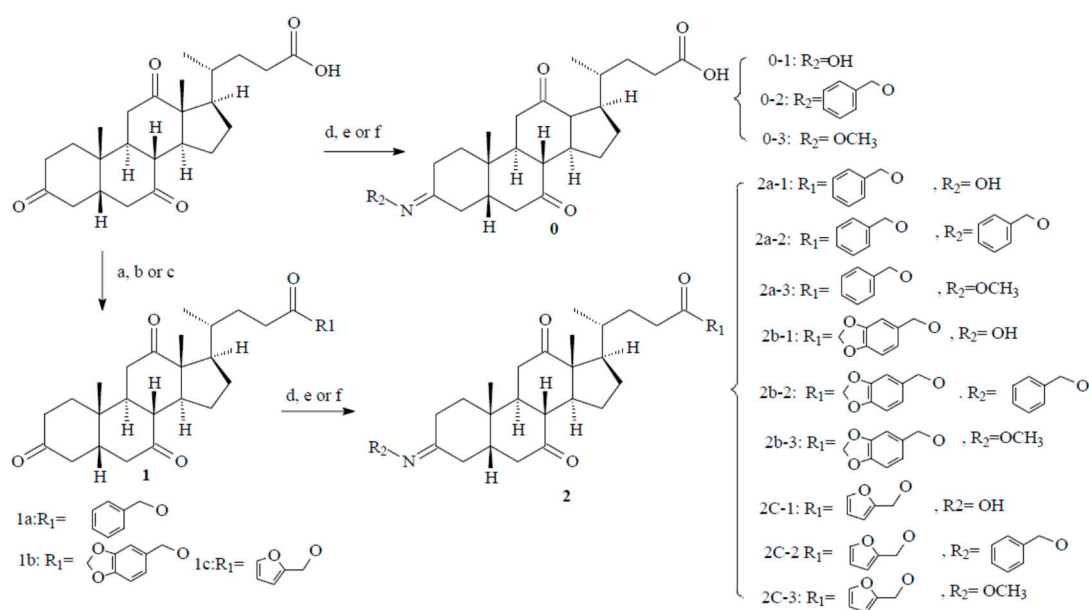
2. Results and Discussion

2.1. Chemistry

The synthetic layout of the intermediates and target compounds is presented in Scheme 1. In the initial step, ester of DHCA 3,7,12-trioxocholanoate (**1a**, **1b** or **1c**) was prepared by DHCA with alcohol (benzyl alcohol, piperonyl alcohol, or furfuryl alcohol) in the presence of *N,N'*-Dicyclohexylcarbodiimide (DCC) in yield of 75.6–76.7%. Then, the intermediates (**1a**, **1b** and **1c**) and DHCA reacted with hydroxylamine, *O*-benzylhydroxylamine, and methoxyamine hydrochloride in DCM with the presence of sodium acetate trihydrate to afford oxime derivatives of DHCA (**2a-1**, **2a-2**, **2a-3**, **2b-1**, **2b-2**, **2b-3**, **2c-1**, **2c-2**, **2c-3**, **0-1**, **0-2**, and **0-3**) as a mixture of isomers. The isomers were easily separated by column chromatography, and the major isomer of these oxime compounds is presumed to have the *E* configuration [31–33]. Structures of these synthesized compounds were elucidated by ¹H NMR, ¹³C NMR, and MS methods. Signals at 211.91–211.96, 209.06–209.09, and 208.71–208.72 ppm in ¹³C NMR spectra of 3, 7, 12-trioxocholanoate were related to the three carbons of C₁₂=O, C₇=O and C₃=O groups, respectively, in the structure of steroid [34]. When C₃=O group was converted to oxime, signals at 208.71–208.72 ppm disappeared and replaced with signals at 156.80–159.40 ppm (C₃=N) in the ¹³C NMR spectra of these compounds, and a broad singlets belonging to the N-OH, N-OCH₂, and N-OCH₃ groups were observed in a range of 7.67–10.23, 4.86–5.00, and 3.68–3.81 (δ in ppm), respectively. The signals at 7.43–6.36 ppm were attributed to protons in the furan ring, 7.01–5.95 ppm to protons in piperonyl group, and 7.54–7.26 ppm to protons in benzyl ring.

2.2. Anti-Hepatitis B Virus (HBV) Activity

A series of oxime derivatives of DHCA were synthesized, and their anti-HBV activities were evaluated with Entecavir (ETV) as the positive control *in vitro* on inhibiting the secretion of HBeAg and HBsAg in HepG2.2.15 cells. Results (Table 1) showed that all compounds were more effective for inhibiting secretion of HBeAg than that of HBsAg. Compounds with significant inhibition of HBeAg secretion were compound **2b-3** (IC₅₀ = 49.39 ± 12.78 μ M, SI = 11.03) and **2b-1** (IC₅₀ = 96.64 ± 28.99 μ M, SI = 10.35) compared to the reference ETV (IC₅₀ = 246.87 ± 50.03 μ M, SI = 2.43), and low cytotoxicity against HepG2.2.15 cell lines (CC₅₀ (**2b-3**) = 544.73 ± 28.92, CC₅₀ (**2b-1**) > 1000 μ M). The other 3 compounds, **2a-1**, **2c-1**, and **0-2**, showed more effective inhibition of HBeAg than ETV's. Apart from these 5 compounds mentioned above, other compounds showed ineffective inhibition of HBeAg secretion, not only with low IC₅₀ values, but also their high cytotoxicity (SI < 1). Only compounds **2a-1** and **2c** group exhibited weak inhibition of HBsAg secretion, and they did not effectively suppress HBV due to their high toxicity (IS < 1).



Scheme 1. Synthetic routes of target compounds. Reagents and conditions: (a) benzyl alcohol, DMAP, DCC/CH₂Cl₂, 0.5 h, 0 °C; overnight, rt; (b) piperonyl alcohol, DMAP, DCC/CH₂Cl₂, 0.5 h, 0 °C; overnight, rt; (c) furfuryl alcohol, DMAP, DCC/CH₂Cl₂, 0.5 h, 0 °C; overnight, rt; (d) NH₂OH·HCl, Sodium acetate trihydrate/CH₂Cl₂, reflux, 3~12 h; (e) NH₂OCH₂C₆H₅·HCl, Sodium acetate trihydrate/CH₂Cl₂, reflux, 3~12 h; (f) NH₂OCH₃·HCl, sodium acetate trihydrate/DCM, reflux, 3~12 h.

Table 1. Cytotoxicity and inhibitory effect of target compounds on HBeAg and HBsAg in vitro.

Compound	CC ₅₀ ^a (μM)	HBeAg ^d		HBsAg ^e	
		IC ₅₀ ^b (μM)	SI ^c	IC ₅₀ ^b (μM)	SI ^c
2a-1	377.88 ± 25.31 **	229.34 ± 12.78	1.65	630.32 ± 34.95 **	0.60
2a-2	210.69 ± 17.11 **	248.66 ± 47.61	0.85	- ^f	-
2a-3	169.10 ± 5.75 **	187.76 ± 9.51	0.90	-	-
2b-1	>1000 **	96.64 ± 28.99 **	10.35	-	-
2b-2	728.15 ± 45.22 *	-	-	-	-
2b-3	544.73 ± 28.92	49.39 ± 12.78 **	11.03	-	-
2c-1	155.05 ± 30.83 **	110.61 ± 28.30 **	1.40	300.00 ± 15.30 **	0.52
2c-2	101.04 ± 10.66 **	151.23 ± 32.11 *	0.67	464.29 ± 20.10 **	0.22
2c-3	90.85 ± 15.59 **	105.19 ± 22.20 **	0.86	180.57 ± 52.83	0.50
0-1	>1000 **	-	-	-	-
0-2	470.47 ± 6.35 *	119.03 ± 1.86 **	3.95	-	-
0-3	>1000 **	-	-	-	-
DHCD ^g	>1000 **	-	-	-	-
ETV ^h	600.12 ± 23.44	246.87 ± 50.03	2.43	161.24 ± 35.94	3.72

^a CC₅₀ is 50% cytotoxicity concentration in HepG 2.2.15 cells; ^b IC₅₀ is 50% inhibitory concentration; ^c SI (selectivity index) = CC₅₀/IC₅₀; ^d HBeAg: hepatitis B e antigen; ^e HBsAg: hepatitis B surface antigen; ^f The inhibition ratio less than 50% in the test concentration range; ^g Dehydrocholic acid (DHCA) is the raw material of reaction; ^h Entecavir (ETV) as the positive control. Data were expressed as mean ± S.D. (n = 3). * Compared with the positive control index: *p* < 0.05. ** Compared with the positive control index: *p* < 0.01.

2.3. Structure–Activity Relationship (SAR)

Results of the bioactive assay showed that DHCA exhibited no activity against the secretion of HBeAg and HBsAg, while most of the derivatives exhibited more or less activity against the secretion of HBsAg and HBeAg, as shown in Table 1.

Five compounds **2a-1**, **2b-1**, **2c-1**, **2b-3**, and **0-2** more effectively inhibited secretion of HBeAg than the positive control ETV. Docking results showed that **2b-1**, **2b-3**, and **0-2** interacted with the HSPG protein with significant docking scores, meanwhile **2a-1** and **2c-1** did not interact with the protein.

Compound **2c-1**, **2c-2**, and **2c-3**, with similar skeletons, but different oxime groups, showed slightly different anti-HBV activity and cytotoxicity. Although with lower IC₅₀ values for inhibiting secretion of HBeAg than oxime **2c-1** and benzyl oxime ether **2c-2**, methyl oxime ether **2c-3** was not an effective inhibitor because of its cytotoxicity (SI = 0.86) (Figure 1). All compounds proved ineffective on inhibiting HBsAg secretion (Figure 2). Bioactive screening results revealed that benzyl oxime ethers (**2a-2**, **2b-2**, and **2c-2**) were less effective (on the base of IC₅₀ values) in inhibiting HBeAg than oximes and methyl oxime ethers. Introduction of a larger group of benzyl to form oxime ethers decreased their inhibition of HBeAg. The results also revealed that oxime derivatives of DHCA eaters (**2a**, **2b**, and **2c**) more effectively inhibited the secretion of HBeAg than the oxime compounds of DHCA (**0-1**, **0-2**, and **0-3**). Results (Table 1) showed that oximes (R₂ = OH), **2a-1**, **2b-1**, and **2c-1** were less toxic in groups **2a**, **2b**, and **2c**, respectively. Methyl ether of oximes **2a-3**, **2b-3**, and **2c-3** were more toxic than others in their groups, respectively. Compound group **c** (**2c-1**, **2c-2**, and **2c-3**), O-furan-2-ylmethyl esters, exhibited obvious more cytotoxicity than benzyl ester (group **2a**), piperonyl esters (group **2b**), and DHCA of oximes (group **0**). These results indicated that formation of O-furan-2-ylmethyl esters increased cytotoxicity of oxime ethers.

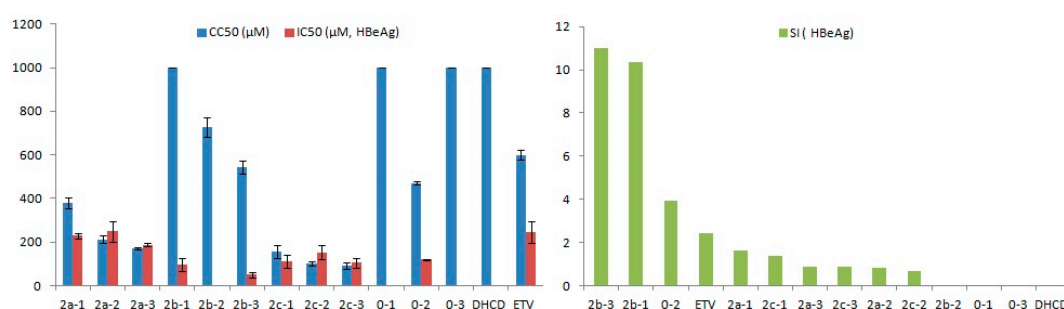


Figure 1. Cytotoxicity, inhibiting HBeAg activity and selectivity index (SI, right) of compounds.

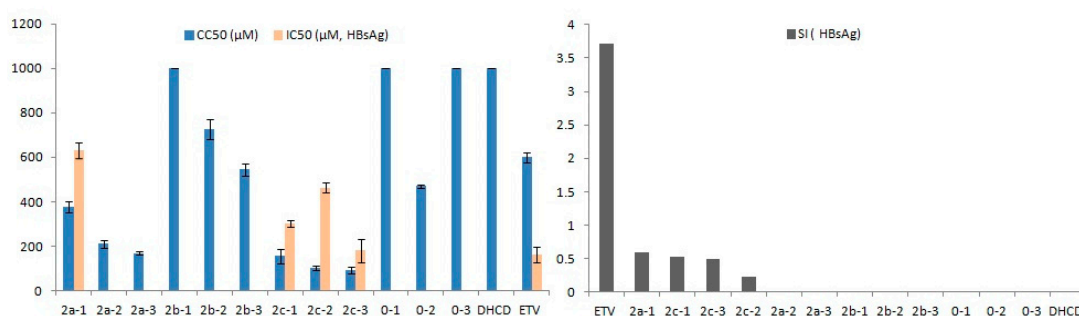


Figure 2. Cytotoxicity, inhibiting HBsAg activity and selectivity index (SI, right) of compounds.

2.4. Molecular Docking Study

To further investigating relationship of structures of the bioactivity and interactions between the ligand and protein of these oxime derivatives, docking studies were carried out using MOE 2008.10. The “Site Finder” tool in this program was used to reach for the active site. Docking study of these oxime derivatives with bile acid receptor protein residue (PDB: 3bej) and HSPG protein residue (PDB: 3sh5) was achieved. The docking scores (S) and the hydrogen bond strength of all the molecules are shown in Tables S2 and S3.

Docking studies showed that DHCA and cholic acid interacted to bile acid receptor with scores in -11.35 and -12.35 kcal/mol, respectively, and bound to residues Lys321 and Ile468 (Figure 3). These results confirmed DHCA possessed hepatocyte targeting activity, theoretically. These oxime derivatives had strong interaction with the dock score ranging from -13.46 to -10.85 kcal/mol with bile acid receptor (Table S2, in Supplementary Material), and -12.54 to -8.43 kcal/mol with HSPG (Table S3, in Supplementary Material), which was very close to the case of cholic acid and DHCA. Moreover, most of the compounds were involved in at least one hydrogen-bonding interaction with bile acid receptor and HSPG.

Bioactive results in vitro showed the compounds **2b-3** and **2b-1** had the most potent anti-HBV activity with IC_{50} values of 49.39 ± 12.78 and 96.64 ± 28.99 μ M for HBeAg, and corresponding SI values of 11.03 and 10.35, respectively. The docking results of protein residue of the bile acid receptor with compounds **2b-3** and **2b-1** showed formation of compound **2b-3** hydrogen bonds length in 2.68 and 3.36 Å for each oxygen atom in the piperonyl group, with Arg 686 and Tyr 397, and 3.00 and 2.83 Å for the oxygen atom of $C_{24}=O$ and $C_{12}=O$ in the ether group and carbonyl group, with Ser 392 and Asn 444 (Figure 4). The results also showed formation of compound **2b-1** hydrogen bonds length in 3.54 and 2.85 Å for one oxygen atom of piperonyl group with Tyr 397 and Gln 396, and 2.92 Å for oxygen atom of $C_{12}=O$ with His 447 (Figure 5). Results of the docking protein residue of HSPG with compound **2b-3** and **2b-1** showed formation of hydrogen bonds length in 2.68 Å for oxygen atom of $C_{12}=O$ of compound **2b-3** with Lys 133, 2.15 Å and 3.16 Å for one oxygen atom of the piperonyl group, with Arg 104, and 2.83 Å for the other oxygen atom of piperonyl group with Val 30 (Figure 6). Similarly, two hydrogen bonds, length 2.31 and 3.25 Å for one oxygen atom of piperonyl group with Arg 104, and 3.22 Å for the other oxygen atom of piperonyl group with Val 30, were found in compound **2b-1** docking results (Figure 7). Contrasting with the **2b-1**, **2b-3**, and **0-2** compounds, **2a-1** and **2c-1** with effective inhibition of HBV showed no interaction to the HSPG protein. These docking results did not coincide with anti-HBV activities. Docking results revealed strong interaction between these oxime derivatives of DHCA and the bile acid receptor, which implied these DHCA derivatives might concentrate to hepatocyte, and possess liver-target activity. Although DHCA and cholic acid docked to the HSPG protein, and showed moderate interactions, they did not exhibit inhibition of HBV in vitro assay (Table S1, Figure S8 in Supplementary Material).

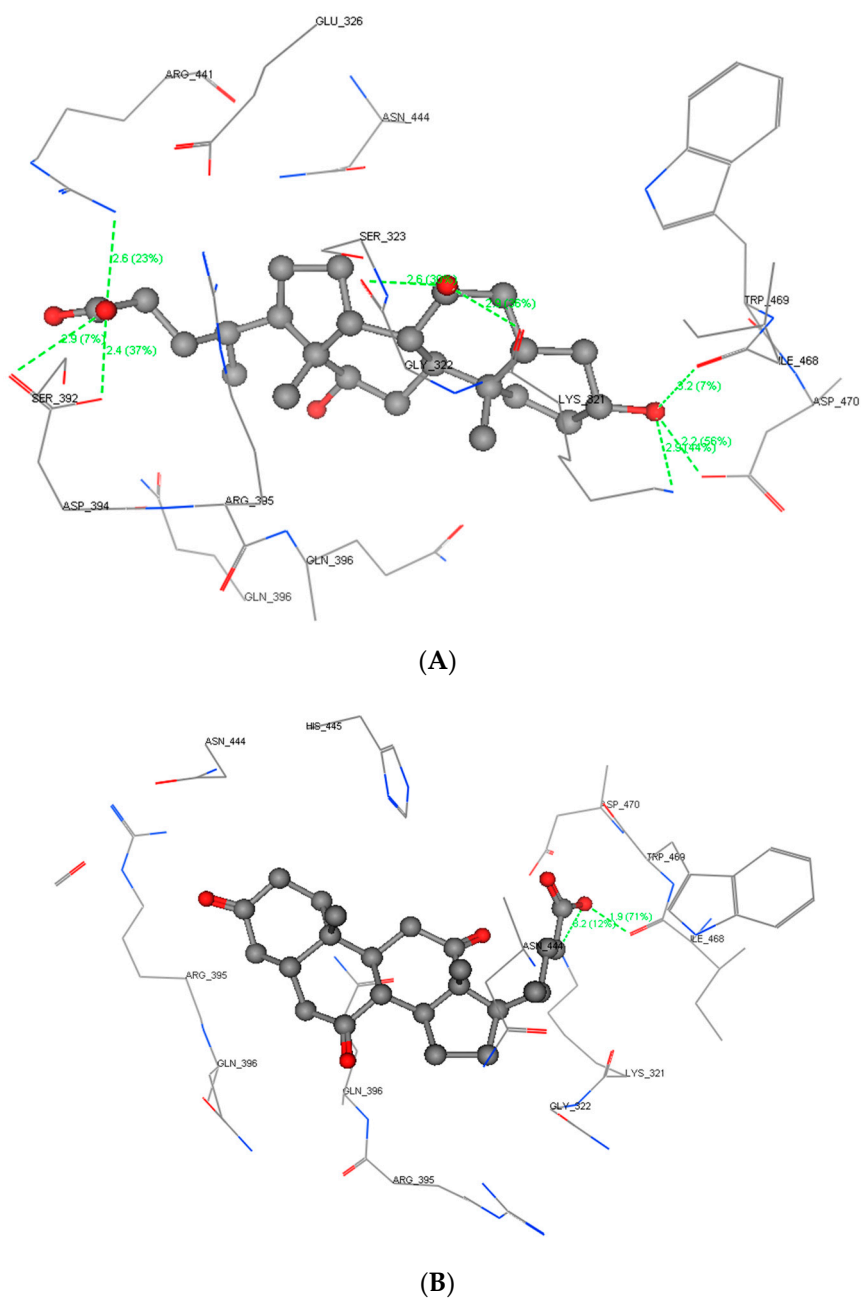


Figure 3. Theoretical Binding mode of compound cholic acid (A) and dehydrocholic acid (B) in bile acid receptor protein (PDB: 3bej) in three-dimensional (3D).

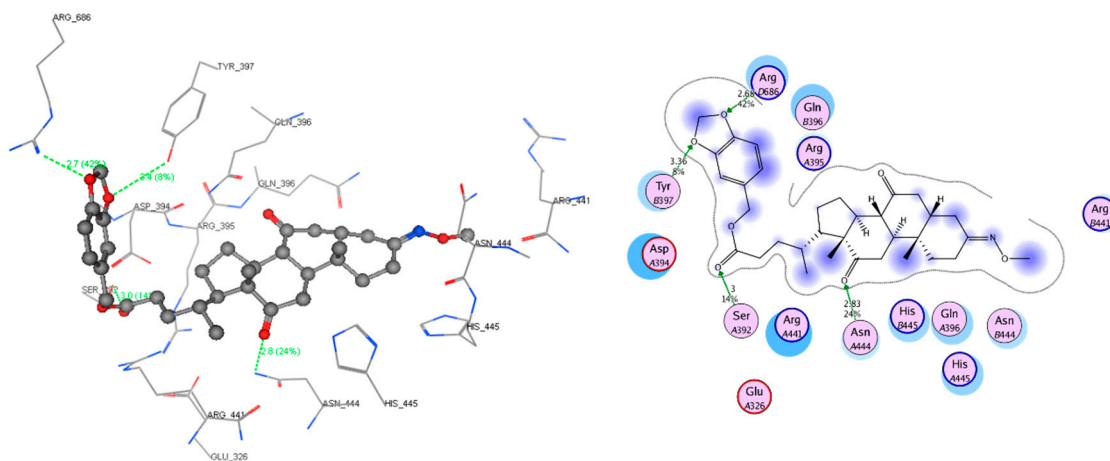


Figure 4. Theoretical Binding mode of compound 2b-3 in bile acid receptor protein (PDB: 3bej) in 3D and two-dimensional (2D).

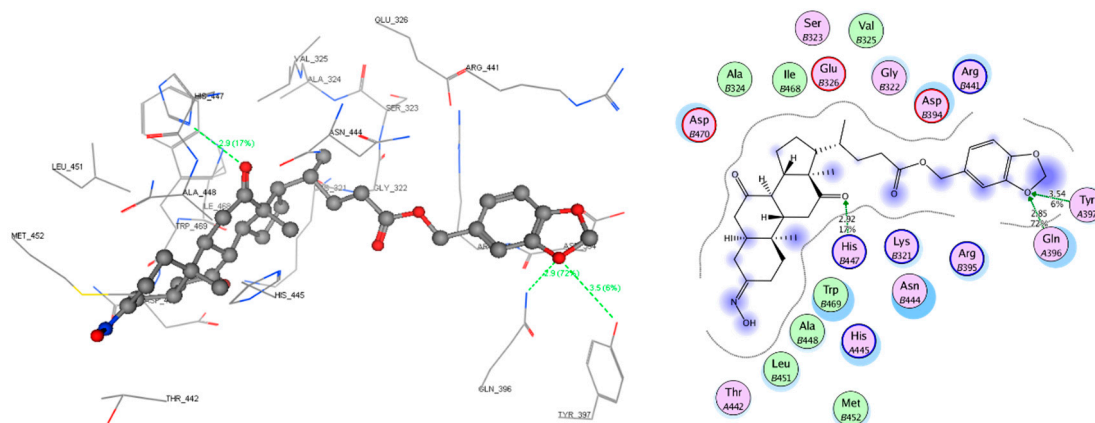


Figure 5. Theoretical Binding mode of compound 2b-1 in bile acid receptor protein (PDB: 3bej) in 3D and 2D.

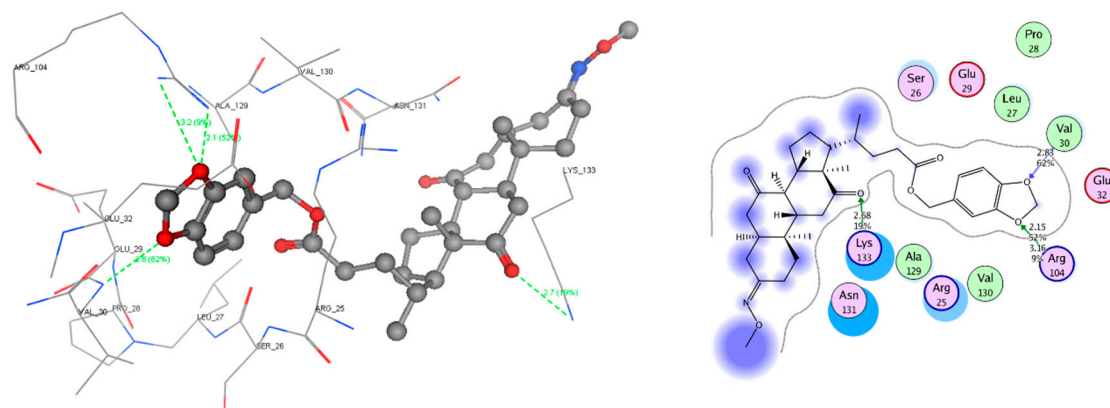


Figure 6. Theoretical Binding mode of compound 2b-3 in heparan sulfate proteoglycan (HSPG) (PDB: 3sh5) in 3D and 2D.

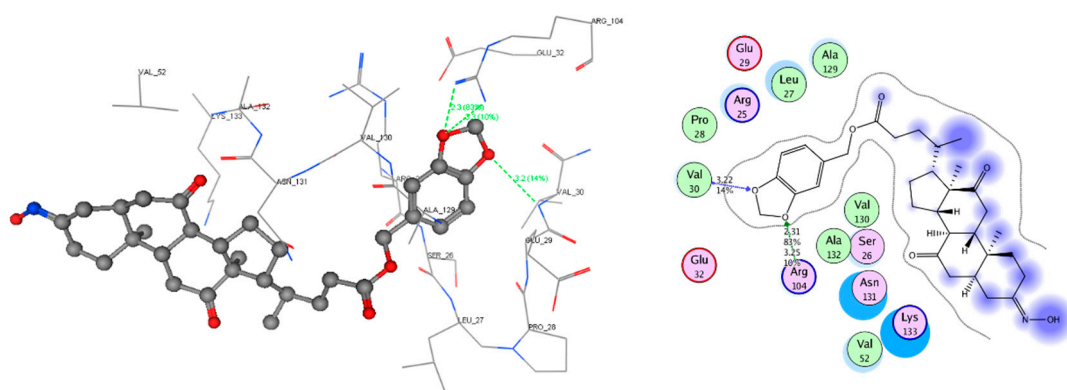


Figure 7. Theoretical Binding mode of compound **2b-1** in HSPG (PDB: 3sh5) in 3D and 2D.

3. Methods

3.1. Synthesis Methods

3.1.1. Chemistry and Chemical Methods

Melting points (mp) were determined on a WRX-4 electrothermal melting point apparatus (Shanghai, China) and were uncorrected. The ^1H NMR and ^{13}C NMR spectra were recorded on a Bruker AV III HD 600 MHz spectrometer using CDCl_3 or $\text{DMSO-}d_6$ as solvent. Chemical shifts were expressed relative to tetramethylsilane (TMS) used as an internal standard and were reported as δ (ppm). The mass spectra were taken on Thermo Scientific ITQ 1100 instrument (Thermo Fisher Scientific, Waltham, MA, USA) with an EIS source and an ion trap analyzer in the positive ion mode. All the reactions were monitored by thin-layer chromatography (TLC) on Silica gel GF-254 plates and the products were separated by flash column chromatography on Silica gel H (Qingdao Haiyang Chemical, Qingdao, China).

3.1.2. General Procedure for the Intermediate Compounds (**1a**, **1b**, and **1c**)

DHCA (1 equiv., 1.25 mmol) and benzyl alcohol, 1,3-benzodioxole-5-methanol, or furfuryl alcohol (1 equiv., 1.25 mmol) were added to a solution of the 4-dimethylaminopyridine (DMAP, 5%) in CH_2Cl_2 (15 mL). The mixture was stirred and cooled to $0\text{ }^\circ\text{C}$ for 0.5 h and then *N,N*-dicyclohexylcarbodiimide (DCC) (1 equiv., 1.25 mmol) was added over a 5-min period. Finally, the reaction was stirred under anhydrous conditions for overnight at room temperature. After stopping, deionized water (4 mL) was added to the resultant solution with lots of white solid (1,3-dicyclohexylurea, DCU) appearing. The mixture was filtered and the filtrate was evaporated to yield a crude product which was purified by column chromatography eluting with an eluent of ethyl acetate/petroleum ether (1:2, *v/v*) to afford **1a**, **1b** and **1c**, respectively.

Benzyl 3,7,12-trioxocholanoate (1a). White crystal, yield 76.5%, mp $203.8\text{--}205.8\text{ }^\circ\text{C}$. ^1H NMR (600 MHz, CDCl_3) δ 7.44–7.28 (5H, m, H-27, 28, 29, 30, 31), 5.13 (2H, q, $J = 12.3$ Hz, H-25), 2.99–2.81 (3H, m, H-6 α , 8 β , 23), 2.53–1.81 (16H, m, H-1 α , 2 β , 4, 5, 6 β , 9, 11, 14, 15 α , 16 β , 17, 22, 23), 1.62 (1H, td, $J = 14.5, 4.5$ Hz, H-20), 1.48–1.22 (7H, m, H-1 β , 2 α , 15 β , 16 α , 18), 1.06 (3H, s, H-19), 0.86 (3H, d, $J = 6.7$ Hz, H-21). ^{13}C NMR (151 MHz, CDCl_3) δ 211.96 (C-12), 209.09 (C-7), 208.72 (C-3), 173.88 (C-24), 136.10 (C-26), 128.55 (C-28, 30), 128.27 (C-27, 31), 128.20 (C-29), 66.12 (C-25), 56.90 (C-17), 51.76 (C-14), 49.00 (C-8), 46.86 (C-9), 45.66 (C-13), 45.56 (C-6), 44.99 (C-5), 42.80 (C-4), 38.63 (C-1), 36.49 (C-2), 36.02 (C-11), 35.46 (C-10), 35.29 (C-20), 31.56 (C-23), 30.46 (C-22), 27.60 (C-15), 25.14 (C-16), 21.92 (C-19), 18.62 (C-21), 11.83 (C-18). ESIMS: m/z 515.2774 [$\text{M} + \text{Na}$] $^+$, calc. for $\text{C}_{31}\text{H}_{40}\text{O}_5$ (492.2876).

3,4-Methylenedioxybenzyl 3,7,12-trioxocholanoate (1b). White crystal, yield 75.6%, mp 209.6~210.6 °C. ¹H NMR (600 MHz, CDCl₃) δ 6.95–6.72 (3H, m, H-27, 28, 31), 5.98 (2H, s, H-32), 5.02 (2H, q, *J* = 12.0 Hz, H-25), 2.98–2.81 (3H, m, H-6α, 8β, 23), 2.47–1.82 (16H, m, H-1α, 2β, 4, 5, 6β, 9, 11, 14, 15α, 16β, 17, 22, 23), 1.62 (1H, td, *J* = 14.5, 4.6 Hz, H-20), 1.46–1.21 (7H, m, H-1β, 2α, 15β, 16α, 18), 1.06 (3H, s, H-19), 0.85 (3H, d, *J* = 6.7 Hz, H-21). ¹³C NMR (151 MHz, CDCl₃) δ 211.93 (C-12), 209.07 (C-7), 208.71 (C-3), 173.86 (C-24), 147.79 (C-30), 147.59 (C-29), 129.88 (C-26), 122.28 (C-27), 109.07 (C-31), 108.23 (C-28), 101.16 (C-32), 66.09 (C-25), 56.89 (C-17), 51.75 (C-14), 49.00 (C-8), 46.85 (C-9), 45.66 (C-13), 45.55 (C-6), 44.99 (C-5), 42.80 (C-4), 38.63 (C-1), 36.49 (C-2), 36.02 (C-11), 35.46 (C-10), 35.29 (C-20), 31.56 (C-23), 30.44 (C-22), 27.61 (C-15), 25.13 (C-16), 21.92 (C-19), 18.62 (C-21), 11.81 (C-18). ESIMS: *m/z* 559.2661 [M + Na]⁺, calc. for C₃₂H₄₀O₇ (536.2774).

Furan-2-ylmethyl 3,7,12-trioxocholanoate (1c). White crystal, yield 76.7%, mp 196.5~198.5 °C. ¹H NMR (600 MHz, CDCl₃) δ 7.40 (1H, d, *J* = 1.7 Hz, H-29), 6.38 (1H, d, *J* = 2.8 Hz, H-27), 6.34 (1H, dd, *J* = 3.2, 1.8 Hz, H-28), 5.04 (2H, q, *J* = 12.3 Hz, H-25), 2.96–2.78 (3H, m, H-6α, 8β, 23), 2.46–1.78 (16H, m, H-1α, 2β, 4, 5, 6β, 9, 11, 14, 15α, 16β, 17, 22, 23), 1.60 (1H, td, *J* = 14.5, 4.5 Hz, H-20), 1.43–1.24 (7H, m, H-1β, 2α, 15β, 16α, 18), 1.03 (3H, s, H-19), 0.81 (3H, d, *J* = 6.7 Hz, H-21). ¹³C NMR (151 MHz, CDCl₃) δ 211.91 (C-12), 209.06 (C-7), 208.71 (C-3), 173.62 (C-24), 149.64 (C-26), 143.20 (C-29), 110.55 (C-28), 110.53 (C-27), 57.87 (C-25), 56.89 (C-17), 51.75 (C-14), 48.99 (C-8), 46.84 (C-9), 45.65 (C-13), 45.54 (C-6), 44.98 (C-5), 42.79 (C-4), 38.63 (C-1), 36.48 (C-2), 36.01 (C-11), 35.45 (C-10), 35.28 (C-20), 31.42 (C-23), 30.38 (C-22), 27.59 (C-15), 25.15 (C-16), 21.91 (C-19), 18.60 (C-21), 11.82 (C-18). ESIMS: *m/z* 505.2559 [M + Na]⁺, calc. for C₂₉H₃₈O₆ (482.2668).

3.1.3. General Procedure for the Target Compounds (2a-1~2a-3, 2b-1~2b-3, 2c-1~2c-3, and 0-1~0-3)

The above intermediate compound **1a**, **1b**, **1c** or DHCA (1 equiv., 0.7mmol) and hydroxylamine, *O*-Benzylhydroxylamine, or methoxyamine hydrochloride (1.3 equiv., 0.91 mmol) was refluxed for 3~12 h with sodium acetate trihydrate (1 equiv., 0.7 mmol) in CH₂Cl₂ (10 mL). After stopping, the mixture was concentrated to give a residue under vacuum. This residue was poured into deionized water with 50% ethanol (30 mL) and extracted with ethyl acetate (2 × 50 mL), and then purified by column chromatography on silica gel eluting with ethyl acetate/petroleum ether (1:6, *v/v*) to give the target compounds.

Benzyl (E)-3-(hydroxyimino)-7,12-dioxocholanoate (2a-1). White crystal, yield 60.3%, mp 199.2~201.2 °C. ¹H NMR (600 MHz, CDCl₃) δ 7.85 (1H, s, -C=N-OH), 7.54–7.30 (5H, m, H-27, 28, 29, 30, 31), 5.13 (2H, q, *J* = 12.3 Hz, H-25), 3.15 (1H, d, *J* = 15.0 Hz, H-2β), 2.96–2.76 (3H, m, H-6α, 8β, 23), 2.51–1.77 (14H, m, H-1α, 4, 5, 6β, 9, 11, 14, 16β, 17, 22, 23), 1.69 (1H, td, *J* = 14.9, 4.5 Hz, H-20), 1.40–1.20 (8H, m, H-1β, 2α, 15, 16α, 18), 1.03 (3H, s, H-19), 0.85 (3H, d, *J* = 6.6 Hz, H-21). ¹³C NMR (151 MHz, CDCl₃) δ 212.77 (C-12), 209.18 (C-7), 173.91 (C-24), 158.55 (C-3), 136.11 (C-26), 128.55 (C-28, 30), 128.26 (C-27, 31), 128.19 (C-29), 66.12 (C-25), 56.95 (C-17), 51.95 (C-14), 48.97 (C-8), 46.42 (C-13), 45.60 (C-9), 45.19 (C-6), 44.97 (C-10), 38.48 (C-11), 36.55 (C-20), 35.46 (C-23), 34.53 (C-22), 33.07 (C-4), 31.57 (C-2), 30.47 (C-15), 27.62 (C-1), 25.24 (C-16), 22.24 (C-21), 19.07 (C-5), 18.61 (C-19), 11.79 (C-18). ESIMS: *m/z* 508.3062 [M + H]⁺, 530.2870 [M + Na]⁺, calc. for C₃₁H₄₁NO₅ (507.2985).

3,4-Methylenedioxybenzyl (E)-3-(hydroxyimino)-7,12-dioxocholanoate (2b-1). White crystal, yield 62.1%, mp 182.5~184.5 °C. ¹H NMR (600 MHz, CDCl₃) δ 7.67 (1H, s, -C=N-OH), 6.99–6.67 (3H, m, H-27, 28, 31), 5.98 (2H, s, H-32), 5.02 (2H, q, *J* = 12.0 Hz, H-25), 3.15 (1H, d, *J* = 15.1 Hz, H-2β), 2.96–2.72 (3H, m, H-6α, 8β, 23), 2.50–1.70 (15H, m, H-1α, 4, 5, 6β, 9, 11, 14, 16β, 17, 20, 22, 23), 1.40–1.23 (8H, m, H-1β, 2α, 15, 16α, 18), 1.04 (3H, s, H-19), 0.85 (3H, d, *J* = 6.7 Hz, H-21). ¹³C NMR (151 MHz, CDCl₃) δ 212.73 (C-12), 209.20 (C-7), 173.92 (C-24), 158.60 (C-3), 147.78 (C-30), 147.58 (C-29), 129.88 (C-26), 122.28 (C-27), 109.07 (C-31), 108.23 (C-28), 101.15 (C-32), 66.09 (C-25), 56.94 (C-17), 51.93 (C-14), 48.97 (C-8), 46.44 (C-13), 45.60 (C-9), 45.20 (C-6), 44.97 (C-10), 38.48 (C-11), 36.55 (C-20), 35.46 (C-23), 34.53 (C-22),

33.06 (C-4), 31.58 (C-2), 30.44 (C-15), 27.62 (C-1), 25.23 (C-16), 22.24 (C-21), 19.06 (C-5), 18.61 (C-19), 11.78 (C-18). ESIMS: m/z 552.2943 [M + H]⁺, 574.2767 [M + Na]⁺, calc. for C₃₂H₄₂NO₇ (551.2883).

Furan-2-ylmethyl (E)-3-(hydroxyimino)-7,12-dioxocholanoate (2c-1). White crystal, yield 60.1%, mp 193.2~195.2 °C. ¹H NMR (600 MHz, CDCl₃) δ 7.72 (1H, s, -C=N-OH), 7.41 (1H, d, *J* = 1.1 Hz, H-29), 6.40 (1H, d, *J* = 3.2 Hz, H-27), 6.36 (1H, dd, *J* = 3.2, 1.9 Hz, H-28), 5.06 (2H, q, *J* = 12.3 Hz, H-25), 3.15 (1H, d, *J* = 15.1 Hz, H-2β), 2.96–2.68 (3H, m, H-6α, 8β, 23), 2.42–1.53 (15H, m, H-1α, 4, 5, 6β, 9, 11, 14, 16β, 17, 20, 22, 23), 1.38–1.19 (8H, m, H-1β, 2α, 15, 16α, 18), 1.03 (3H, s, H-19), 0.82 (3H, d, *J* = 6.7 Hz, H-21). ¹³C NMR (151 MHz, CDCl₃) δ 212.38 (C-12), 209.11 (C-7), 173.67 (C-24), 158.19 (C-3), 149.63 (C-26), 143.19 (C-29), 110.54 (C-28), 110.52 (C-27), 57.87 (C-25), 56.87 (C-17), 51.79 (C-14), 48.98 (C-8), 45.61 (C-9), 45.36 (C-13), 45.32 (C-6), 45.05 (C-10), 38.50 (C-11), 36.53 (C-20), 35.63 (C-5), 35.46 (C-23), 31.43 (C-2), 30.39 (C-15), 27.60 (C-1), 26.25 (C-22), 25.64 (C-4), 25.20 (C-16), 22.33 (C-21), 18.60 (C-19), 11.80 (C-18). ESIMS: m/z 498.2839 [M + H]⁺, 520.2668 [M + Na]⁺, calc. for C₂₉H₃₉NO₆ (497.2777).

Benzyl (E)-3-((benzyloxy)imino)-7,12-dioxocholanoate (2a-2). White solid, yield 50.9%, mp 135.3~137.3 °C. ¹H NMR (600 MHz, CDCl₃) δ 7.39–7.26 (10H, m, H-27, 28, 29, 30, 31, 34, 35, 36, 37, 38), 5.11 (2H, q, *J* = 12.3 Hz, H-25), 5.06–5.00 (2H, m, H-32), 3.13 (1H, d, *J* = 14.9 Hz, H-2β), 2.94–2.67 (3H, m, H-6α, 8β, 23), 2.47–1.62 (15H, m, H-1α, 4, 5, 6β, 9, 11, 14, 16β, 17, 20, 22, 23), 1.36–1.16 (8H, m, H-1β, 2α, 15, 16α, 18), 1.01 (3H, s, H-19), 0.83 (3H, d, *J* = 6.7 Hz, H-21). ¹³C NMR (151 MHz, CDCl₃) δ 212.31 (C-12), 209.10 (C-7), 173.88 (C-24), 158.30 (C-3), 138.01 (C-33), 136.12 (C-26), 128.55 (C-35, 37), 128.33 (C-28, 30), 128.27 (C-34, 38), 128.19 (C-29), 127.93 (C-27, 31), 127.69 (C-36), 75.36 (C-32), 66.11 (C-25), 56.88 (C-17), 51.85 (C-14), 48.93 (C-8), 46.57 (C-13), 45.62 (C-9), 45.20 (C-6), 44.99 (C-10), 38.49 (C-11), 36.52 (C-20), 35.47 (C-23), 34.67 (C-22), 33.16 (C-4), 31.57 (C-2), 30.48 (C-15), 27.63 (C-1), 25.22 (C-16), 22.24 (C-21), 20.20 (C-5), 18.62 (C-19), 11.80 (C-18). ESIMS: m/z 598.3533 [M + H]⁺, calc. for C₃₈H₄₇NO₅ (597.3454).

3,4-Methylenedioxybenzyl (E)-3-((benzyloxy)imino)-7,12-dioxocholanoate (2b-2). White solid, yield 51.1%, mp 124.3~126.3 °C. ¹H NMR (600 MHz, CDCl₃) δ 7.39–7.28 (5H, m, H-34, 35, 36, 37, 38, 39), 7.01–6.71 (3H, m, H-27, 28, 31), 5.98 (2H, s, H-32), 5.18–4.86 (4H, m, H-25, 33), 3.15 (1H, d, *J* = 15.0 Hz, H-2β), 2.95–2.74 (3H, m, H-6α, 8β, 23), 2.49–1.64 (15H, m, H-1α, 4, 5, 6β, 9, 11, 14, 16β, 17, 20, 22, 23), 1.39–1.24 (8H, m, H-1β, 2α, 15, 16α, 18), 1.04 (3H, s, H-19), 0.85 (3H, d, *J* = 6.7 Hz, H-21). ¹³C NMR (151 MHz, CDCl₃) δ 212.29 (C-12), 209.10 (C-7), 173.88 (C-24), 158.30 (C-3), 147.79 (C-30), 147.59 (C-29), 138.01 (C-34), 129.89 (C-37), 128.33 (C-36, 38), 127.93 (C-35, 39), 127.69 (C-26), 122.28 (C-27), 109.07 (C-31), 108.23 (C-28), 101.16 (C-32), 75.36 (C-33), 66.08 (C-25), 56.87 (C-17), 51.85 (C-14), 48.93 (C-8), 46.57 (C-13), 45.61 (C-9), 45.20 (C-6), 44.99 (C-10), 38.49 (C-11), 36.52 (C-20), 35.48 (C-23), 34.67 (C-22), 33.16 (C-4), 31.58 (C-2), 30.46 (C-15), 27.63 (C-1), 25.22 (C-16), 22.24 (C-21), 20.20 (C-5), 18.62 (C-19), 11.79 (C-18). ESIMS: m/z 664.3219 [M + Na]⁺, calc. for C₃₉H₄₇NO₇ (641.3353).

Furan-2-ylmethyl (E)-3-((benzyloxy)imino)-7,12-dioxocholanoate (2c-2). White solid, yield 51.5%, mp 131.5~133.5 °C. ¹H NMR (600 MHz, CDCl₃) δ 7.43 (1H, d, *J* = 1.0 Hz, H-29), 7.38–7.28 (5H, m, H-32, 33, 34, 35, 36), 6.42 (1H, d, *J* = 3.1 Hz, H-27), 6.38 (1H, dd, *J* = 2.9, 1.9 Hz, H-28), 5.31–4.80 (4H, m, H-25, 30), 3.15 (1H, d, *J* = 15.1 Hz, H-2β), 2.95–2.72 (3H, m, H-6α, 8β, 23), 2.49–1.64 (15H, m, H-1α, 4, 5, 6β, 9, 11, 14, 16β, 17, 20, 22, 23), 1.40–1.24 (8H, m, H-1β, 2α, 15, 16α, 18), 1.04 (3H, s, H-19), 0.84 (3H, d, *J* = 6.6 Hz, H-21). ¹³C NMR (151 MHz, CDCl₃) δ 212.31 (C-12), 209.12 (C-7), 173.66 (C-24), 158.31 (C-3), 149.65 (C-26), 143.20 (C-29), 138.00 (C-31), 128.33 (C-33, 35), 127.93 (C-32, 36), 127.69 (C-34), 110.55 (C-28), 110.53 (C-27), 75.36 (C-30), 57.87 (C-25), 56.88 (C-17), 51.85 (C-14), 48.93 (C-8), 46.57 (C-13), 45.61 (C-9), 45.19 (C-6), 44.99 (C-10), 38.49 (C-11), 36.52 (C-20), 35.47 (C-23), 34.67 (C-22), 33.15 (C-4), 31.44 (C-2), 30.40 (C-15), 27.61 (C-1), 25.24 (C-16), 22.24 (C-21), 20.20 (C-5), 18.60 (C-19), 11.80 (C-18). ESIMS: m/z 588.3301 [M + H]⁺, 610.3130 [M + Na]⁺, calc. for C₃₆H₄₅NO₆ (587.3247).

Benzyl (E)-3-(methoxyimino)-7,12-dioxolcholanoate (2a-3). White solid, yield 61.5%, mp 132.6~134.6 °C. ¹H NMR (600 MHz, CDCl₃) δ 7.45–7.29 (5H, m, H-27, 28, 29, 30, 31), 5.13 (2H, q, *J* = 12.3 Hz, H-25), 3.81 (3H, s, H-32), 3.06 (1H, d, *J* = 15.1 Hz, H-2β), 2.96–2.72 (3H, m, H-6α, 8β, 23), 2.53–1.64 (15H, m, H-1α, 4, 5, 6β, 9, 11, 14, 16β, 17, 20, 22, 23), 1.40–1.22 (8H, m, H-1β, 2α, 15, 16α, 18), 1.03 (3H, s, H-19), 0.86 (3H, d, *J* = 6.7 Hz, H-21). ¹³C NMR (151 MHz, CDCl₃) δ 212.31 (C-12), 209.12 (C-7), 173.88 (C-24), 157.64 (C-3), 136.12 (C-26), 128.55 (C-28, 30), 128.22 (C-27, 31), 128.19 (C-29), 66.10 (C-25), 61.18 (C-32), 56.88 (C-17), 51.84 (C-24), 48.94 (C-8), 46.64 (C-13), 45.62 (C-9), 45.21 (C-6), 45.00 (C-10), 38.49 (C-11), 36.54 (C-20), 35.47 (C-23), 34.69 (C-22), 33.17 (C-4), 31.57 (C-2), 30.48 (C-15), 27.62 (C-1), 25.21 (C-16), 22.26 (C-21), 19.89 (C-5), 18.62 (C-19), 11.80 (C-18). ESIMS: *m/z* 522.3220 [M + H]⁺, 544.3052 [M + Na]⁺, calc. for C₃₂H₄₃NO₅ (521.3141).

3,4-Methylenedioxybenzyl (E)-3-(methoxyimino)-7,12-dioxocholanoate (2b-3). White solid, yield 62.2%, mp 118.7~120.7 °C. ¹H NMR (600 MHz, CDCl₃) δ 6.89–6.69 (3H, m, H-27, 28, 31), 5.95 (2H, s, H-32), 5.00 (2H, q, *J* = 12.0 Hz, H-25), 3.78 (3H, s, H-33), 3.03 (1H, d, *J* = 14.9 Hz, H-2β), 2.93–2.70 (3H, m, H-6α, 8β, 23), 2.44–1.62 (15H, m, H-1α, 4, 5, 6β, 9, 11, 14, 16β, 17, 20, 22, 23), 1.39–1.22 (8H, m, H-1β, 2α, 15, 16α, 18), 1.01 (3H, s, H-19), 0.82 (3H, d, *J* = 6.6 Hz, H-21). ¹³C NMR (151 MHz, CDCl₃) δ 212.30 (C-12), 209.12 (C-7), 173.88 (C-24), 157.64 (C-3), 147.78 (C-30), 147.58 (C-29), 129.89 (C-26), 122.27 (C-27), 109.07 (C-31), 108.23 (C-28), 101.15 (C-32), 66.07 (C-25), 61.17 (C-33), 56.88 (C-17), 51.84 (C-14), 48.94 (C-8), 46.63 (C-13), 45.61 (C-9), 45.20 (C-6), 45.00 (C-10), 38.49 (C-11), 36.54 (C-20), 35.47 (C-23), 34.69 (C-22), 33.17 (C-4), 31.57 (C-2), 30.46 (C-15), 27.63 (C-1), 25.21 (C-16), 22.26 (C-21), 19.89 (C-5), 18.62 (C-19), 11.79 (C-18). ESIMS: *m/z* 566.3123 [M + H]⁺, 588.2953 [M + Na]⁺, calc. for C₃₃H₄₃NO₇ (565.3040).

Furan-2-ylmethyl (E)-3-(methoxyimino)-7,12-dioxocholanoate (2c-3). White solid, yield 60.8%, mp 122.3~124.3 °C. ¹H NMR (600 MHz, CDCl₃) δ 7.43 (1H, d, *J* = 1.2 Hz, H-29), 6.41 (1H, d, *J* = 3.2 Hz, H-27), 6.37 (1H, dd, *J* = 3.1, 1.9 Hz, H-28), 5.07 (2H, q, *J* = 12.3 Hz, H-25), 3.80 (3H, s, H-30), 3.06 (1H, d, *J* = 15.5 Hz, H-2β), 2.96–2.73 (3H, m, H-6α, 8β, 23), 2.48–1.65 (15H, m, H-1α, 4, 5, 6β, 9, 11, 14, 16β, 17, 20, 22, 23), 1.42–1.26 (8H, m, H-1β, 2α, 15, 16α, 18), 1.04 (3H, s, H-19), 0.84 (3H, d, *J* = 6.7 Hz, H-21). ¹³C NMR (151 MHz, CDCl₃) δ 212.31 (C-12), 209.13 (C-7), 173.66 (C-24), 157.65 (C-3), 149.65 (C-26), 143.20 (C-29), 110.55 (C-28), 110.52 (C-27), 61.16 (C-30), 57.87 (C-25), 56.88 (C-17), 51.77 (C-14), 48.94 (C-8), 46.64 (C-13), 45.62 (C-9), 45.20 (C-6), 45.00 (C-10), 38.50 (C-11), 36.54 (C-6), 35.47 (C-23), 34.69 (C-22), 33.17 (C-4), 31.44 (C-2), 30.40 (C-15), 27.61 (C-1), 25.23 (C-16), 22.26 (C-21), 19.89 (C-5), 18.61 (C-19), 11.80 (C-18). ESIMS: *m/z* 534.2811 [M + Na]⁺, calc. for C₃₀H₄₁NO₆ (511.2934).

(E)-3-(hydroxyimino)-7,12-dioxolcholanic acid (0-1). White solid, yield 63.8%, mp 250.4~252.4 °C. ¹H NMR (600 MHz, DMSO-*d*₆) δ 10.23 (1H, s, -C=N-OH), 3.07–2.78 (4H, m, H-2β, 6α, 8β, 23), 2.35–1.40 (15H, m, H-1α, 4, 5, 6β, 9, 11, 14, 16β, 17, 20, 22, 23), 1.30–1.20 (8H, m, H-1β, 2α, 15, 16α, 18), 0.99 (3H, s, H-19), 0.76 (3H, d, *J* = 5.5 Hz, H-21). ¹³C NMR (151 MHz, DMSO-*d*₆) δ 212.60 (C-12), 210.21 (C-7), 175.31 (C-24), 156.80 (C-3), 56.68 (C-17), 51.78 (C-14), 48.42 (C-8), 46.53 (C-13), 45.82 (C-9), 45.27 (C-6), 45.23 (C-10), 44.63 (C-5), 38.72 (C-11), 36.69 (C-20), 35.46 (C-23), 34.64 (C-22), 33.30 (C-4), 31.59 (C-2), 30.85 (C-15), 27.69 (C-1), 25.07 (C-16), 22.29 (C-21), 19.14 (C-19), 11.89 (C-18). ESIMS: *m/z* 418.2581 [M + H]⁺, 440.2403 [M + Na]⁺, calc. for C₂₄H₃₅NO₅ (417.2515).

(E)-3-((benzyloxy)imino)-7,12-dioxolcholanic acid (0-2). White solid, yield 51.2%, mp 198.5~200.5 °C. ¹H NMR (600 MHz, DMSO-*d*₆) δ 11.95 (1H, s, -COOH), 7.56–7.00 (5H, m, H-27, 28, 29, 30, 31), 4.97 (2H, s, H-25), 3.06–2.73 (4H, m, H-2β, 6α, 8β, 23), 2.42–1.52 (15H, m, H-1α, 4, 5, 6β, 9, 11, 14, 16β, 17, 20, 22, 23), 1.28–1.15 (8H, m, H-1β, 2α, 15, 16α, 18), 0.99 (3H, s, H-19), 0.76 (3H, d, *J* = 6.1 Hz, H-21). ¹³C NMR (151 MHz, DMSO-*d*₆) δ 212.48 (C-12), 210.12 (C-7), 175.26 (C-24), 159.40 (C-3), 138.77 (C-26), 128.70 (C-28, 30), 128.18 (C-27, 31), 128.05 (C-29), 74.71 (C-25), 56.68 (C-17), 51.70 (C-14), 48.37 (C-8), 46.47 (C-13), 45.83 (C-9), 45.20 (C-6), 44.96 (C-10), 44.29 (C-5), 38.65 (C-11), 36.62 (C-20), 35.47 (C-23),

34.59 (C-22), 33.02 (C-4), 31.56 (C-2), 30.84 (C-15), 27.70 (C-1), 25.11 (C-16), 22.05 (C-21), 19.15 (C-19), 11.88 (C-18). ESIMS: m/z 508.3042 $[M + H]^+$, 530.2865 $[M + Na]^+$, calc. for $C_{31}H_{41}NO_5$ (507.2985).

(*E*)-3-(methoxyimino)-7,12-dioxolcholanolic acid (**0-3**). White solid, yield 61.3%, mp 197.2~199.2 °C. 1H NMR (600 MHz, $DMSO-d_6$) δ 11.96 (1H, s, -COOH), 3.68 (3H, s, H-25), 3.05–2.73 (4H, m, H-2 β , 6 α , 8 β , 23), 2.41–1.45 (15H, m, H-1 α , 4, 5, 6 β , 9, 11, 14, 16 β , 17, 20, 22, 23), 1.29–1.13 (8H, m, H-1 β , 2 α , 15, 16 α , 18), 0.99 (3H, s, H-19), 0.76 (3H, d, $J = 5.4$ Hz, H-21). ^{13}C NMR (151 MHz, $DMSO-d_6$) δ 212.48 (C-12), 210.13 (C-7), 175.30 (C-24), 158.62 (C-3), 60.98 (C-25), 56.68 (C-17), 51.71 (C-14), 48.37 (C-8), 46.51 (C-13), 45.83 (C-9), 45.23 (C-6), 44.99 (C-10), 44.33 (C-5), 38.66 (C-11), 36.65 (C-20), 35.47 (C-23), 34.60 (C-22), 32.98 (C-4), 31.60 (C-2), 30.86 (C-15), 27.70 (C-1), 25.09 (C-16), 22.07 (C-21), 19.15 (C-19), 11.88 (C-18). ESIMS: m/z 454.2575 $[M + Na]^+$, calc. for $C_{25}H_{37}NO_5$ (431.2672).

3.2. Biological Evaluation Methods

3.2.1. Cell Culture and Drug Treatment

HepG2.2.15 cells were kindly provided by the Chinese Academy of Medical Sciences (Beijing, China), derived from human hepatoma cell line G2. These cells were cultured in Dulbecco's Modified Eagle's Medium (DMEM), supplemented with 10% fetal bovine serum (FBS), 1.5 g/L of sodium bicarbonate, 10 mL/L of penicillin, and streptomycin, respectively, and 200 mg/L of G418 at 37 °C under 5% carbon dioxide in a 95–98% humidity. The compounds were diluted to the desired concentrations in culture medium. Before treated with various concentrations of compounds, cells were seeded at a density of 1×10^5 cells/mL in 96-well plates and incubated for 24 h at 37 °C. Every three days in a nine day period, supernatant of each well was replaced with compound-containing fresh medium [23].

3.2.2. Method for Cell Toxicity and HBsAg and HBeAg Inhibition Assays

The levels of HBeAg and HBsAg in the supernatant of the cells were measured using ELISA assay following the manufacturer's protocol (Shanghai Kehua Bio-engineering Co., Ltd., Shanghai, China). The synthesized compounds were expressed as the concentration that achieved 50% inhibition (IC_{50}) to the secretion of HBeAg and HBsAg [29].

The cytotoxicity activity of the synthesized compounds was determined by MTT assay [35]. After refreshing the supernatant, 20 μ L MTT (5 mg/mL) was added to each well, which was further cultured for 4 h at 37 °C. Then the supernatant of each well was carefully removed, formazan crystals were dissolved in 150 μ L of DMSO and the absorbance at 450 nm was recorded [36]. Cytotoxicity of these compounds was expressed as the concentration of compound required to kill 50% (CC_{50}) of the HepG2.2.15 cells.

3.3. Molecular Docking

The crystal structures of heparan sulfate proteoglycan (HSPG) protein (P98160, PDB: 3sh5) and bile acid receptor protein (Q96RI1, PDB:3bej) were downloaded from The UniProt Knowledgebase (<https://www.uniprot.org/>). Molecular Docking simulations of the compounds inside the protein, which from HSPG and bile acid receptor, were carried out by using Molecular Operating Environment (MOE) 2008.10. Initially, structures of compounds were protonated with addition of polar hydrogens, and then converted to three-dimensional (3D) structures, followed by energy minimization with force-field using HyperChem 8.0.7 to get stabilized conformers. The stabled conformer of compounds were introduced to MOE, and then proceeded an "energy minimize" process to offer structurally optimized compounds, and were saved as PDB format files, respectively. After crystal structures of the receptor protein were introduced to MOE, unbound water, other small molecules, and ions were removed, then "protonate 3D" was proceeded, to add protons to the proteins, subsequently followed by an "energy minimize" process to give structurally optimized protein. A structurally optimized compound was then introduced to optimized protein to proceed docking simulation. Docking score

and interaction sites, types, and distances, along with two-dimensional (2D) and 3D interaction diagrams, were obtained with the MOE method.

4. Conclusions

As a part of our series of works for exploring anti-HBV agents, a series of non-nucleoside anti-HBV compounds, by attaching the oximes to dehydrocholic acid (DHCA), have been designed, synthesized, and screened for their bioactivity. Five compounds were found with more effective inhibition of HBeAg than the positive control ETV, two of them, **2b-3** and **2b-1**, showed significant anti-HBV activities against the secretion of HBeAg ($IC_{50(2b-3)} = 49.39 \pm 12.78$, $SI_{2b-3} = 11.03$ and $IC_{50(2b-1)} = 96.64 \pm 28.99 \mu\text{M}$, $SI_{2b-1} = 10.35$). Results of the molecular docking study showed that there are strong interactions between these compounds and bile acid receptor and HSPG.

Supplementary Materials: The following are available online.

Author Contributions: Z.W. and J.T. performed the experiments, analyzed results and wrote this paper; M.Z., X.C. and Y.H. took part in synthesis of compounds and molecular design; N.Z. and Z.C. performed molecular docking and took part in bioactive assay. W.W. conceived and supervised the project. All authors have read and agreed to the published version of the manuscript.

Funding: Financial support from the National Natural Science Foundation of China (No. 81760635) is gratefully acknowledged.

Conflicts of Interest: The authors have no relevant affiliations or financial involvement with any organization or entity with a financial interest in or financial conflict with the subject matter or materials discussed in the manuscript. This includes employment, consultancies, honoraria, stock ownership or options, expert testimony, grants or patents received or pending, or royalties. The funders had no role in the design of the study; in the collection, analyses, or interpretation of data; in the writing of the manuscript, or in the decision to publish the results.

References

1. You, C.R.; Lee, S.W.; Jang, J.W.; Yoon, S.K. Update on hepatitis B virus infection. *World J. Gastroenterol.* **2014**, *20*, 13293–13305. [CrossRef] [PubMed]
2. Lin, C.L.; Kao, J.H. Risk stratification for hepatitis B virus related hepatocellular carcinoma. *J. Gastroenterol. Hepatol.* **2013**, *28*, 10–17. [CrossRef] [PubMed]
3. World Health Organization (WHO). Global Hepatitis Report 2017. Available online: <https://apps.who.int/iris/bitstream/handle/10665/255016/9789241565455-eng.pdf> (accessed on 4 July 2017).
4. Dienstag, J.L.; Schiff, E.R.; Wright, T.L.; Perrillo, R.P.; Hann, H.W.L.; Goodman, Z.; Crowther, L.; Condreay, L.D.; Woessner, M.; Rubin, M.; et al. Lamivudine as initial treatment for chronic hepatitis B in the United States. *N. Engl. J. Med.* **1999**, *341*, 1256–1263. [CrossRef] [PubMed]
5. Torresi, J.; Locarnini, S. Antiviral chemotherapy for the treatment of hepatitis b virus infections. *Gastroenterology* **2000**, *118*, S83–S103. [CrossRef]
6. Gish, R.G.; Lai, C.; Yuen, M. Entecavir: A Review of its Use in the Treatment of Chronic Hepatitis B in Patients with Decompensated Liver Disease. *Drugs* **2011**, *71*, 2511–2529.
7. Seifer, M.; Hamatake, R.K.; Colonno, R.J.; Stranding, D.N. In Vitro Inhibition of Hepadnavirus Polymerases by the Triphosphates of BMS-200475 and Lobucavir, *Antimicrob. Agents Chemoth.* **1998**, *42*, 3200–3208. [CrossRef]
8. Ghany, M.G.; Doo, E.C. Antiviral Resistance and Hepatitis B Therapy. *Hepatology* **2009**, *49*, S174–S184. [CrossRef]
9. Zoulim, F.; Poynard, T.; Degos, F.; Slama, A.; Hasnaoui El, A.; Blin, P.; Mercier, F.; Deny, P.; Landais, P.; Parvaz, P.; et al. A prospective study of the evolution of lamivudine resistance mutations in patients with chronic hepatitis B treated with lamivudine. *J. Viral Hepat.* **2006**, *13*, 278–288. [CrossRef]
10. Yang, X.Y.; Xu, X.Q.; Guan, H.; Wang, L.L.; Wu, Q.; Wu, G.M.; Li, S. A new series of HAPs as anti-HBV agents targeting at capsid assembly. *Bioorg. Med. Chem. Lett.* **2014**, *24*, 4247–4249. [CrossRef]
11. Zembower, D.E.; Lin, Y.M.; Flavin, M.T.; Chen, F.C.; Korba, B.E. Robustaflavone, a potential non-nucleoside anti-hepatitis B agent. *Antivir. Res.* **1998**, *39*, 81–88. [CrossRef]

12. Wei, W.X.; Li, X.R.; Wang, K.W.; Zheng, Z.W.; Zhou, M. Lignans with anti-hepatitis B virus activities from *Phyllanthus niruri* L. *Phytother. Res.* **2012**, *26*, 964–968. [[CrossRef](#)] [[PubMed](#)]
13. Liu, S.; Wei, W.X.; Shi, K.C.; Cao, X.; Zhou, M.; Liu, Z.P. In vitro and in vivo anti-hepatitis B virus activities of the lignan niranthin isolated from *Phyllanthus niruri* L. *J. Ethnopharmacol.* **2014**, *155*, 1061–1067. [[CrossRef](#)] [[PubMed](#)]
14. Zhan, P.; Jiang, X.M.; Liu, X.Y. Naturally Occurring and Synthetic Bioactive Molecules as Novel Non-Nucleoside HBV Inhibitors. *Mini-Rev. Med. Chem.* **2010**, *10*, 162–171. [[CrossRef](#)] [[PubMed](#)]
15. Zhang, F.; Wang, G. A review of non-nucleoside anti-hepatitis B virus agents. *Eur. J. Med. Chem.* **2014**, *75*, 267–281. [[CrossRef](#)]
16. Yang, W.; Peng, Y.M.; Wang, J.W.; Song, C.J.; Yu, W.Q.; Zhou, Y.B.; Jiang, J.H.; Wang, Q.D.; Wu, J.; Chang, J.B. Design, synthesis, and biological evaluation of novel 2'-deoxy-2'-fluoro-2'-C-methyl 8-azanebularine derivatives as potent anti-HBV agents. *Bioorg. Med. Chem. Lett.* **2019**, *29*, 1291–1297. [[CrossRef](#)] [[PubMed](#)]
17. Ivashchenko, A.V.; Mitkin, O.D.; Kravchenko, D.V.; Kuznetsova, I.V.; Kovalenko, S.M.; Bunyatyan, N.D.; Langer, T. Synthesis, X-Ray Crystal Structure, Hirshfeld Surface Analysis, and Molecular Docking Study of Novel Hepatitis B (HBV) Inhibitor: 8-Fluoro-5-(4-fluorobenzyl)-3-(2-methoxybenzyl)-3,5-dihydro-4H-pyrimido[5, 4-b]indol-4-one. *Heliyon* **2019**, *2019*, e02738. [[CrossRef](#)]
18. Liu, S.; Li, Y.B.; Wei, W.X.; Wang, K.W.; Wang, L.S.; Wang, J.Y. Design, Synthesis, Molecular Docking Studies and Anti-HBV Activity of Phenylpropanoid Derivatives. *Chemico-Biol. Interact.* **2016**, *25*, 1–9. [[CrossRef](#)]
19. Zhao, S.M.; Zhen, Y.Q.; Fu, L.L.; Gao, F.; Zhou, X.L.; Huang, S.; Zhang, L. Design, synthesis and biological evaluation of benzamide derivatives as novel NTCP inhibitors that induce apoptosis in HepG2 cells. *Bioorg. Med. Chem. Lett.* **2019**, *29*, 126623. [[CrossRef](#)]
20. Vandyck, K.; Rombouts, G.; Stoops, B.; Tahri, A.; Vos, A.; Verschuere, W.; Wu, Y.; Yang, J.; Hou, F.; Huang, B.; et al. Synthesis and evaluation of N-phenyl-3-sulfamoyl-benzamide derivatives as capsid assembly modulators inhibiting hepatitis B virus (HBV). *J. Med. Chem.* **2018**, *61*, 6247–6260.
21. Li, T.; Li, J.; Yang, Y.; Han, Y.L.; Wu, D.R.; Xiao, T.; Wang, Y.; Liu, T.; Zhao, Y.L.; Li, Y.J.; et al. Synthesis, pharmacological evaluation, and mechanistic study of adefovir mixed phosphonate derivatives bearing cholic acid and L-amino acid moieties for the treatment of HBV. *Bioorg. Med. Chem.* **2019**, *27*, 3707–3721. [[CrossRef](#)] [[PubMed](#)]
22. Li, W. The Hepatitis B Virus Receptor. *Ann. Rev. Cell Develop. Biol.* **2015**, *31*, 125–147. [[CrossRef](#)] [[PubMed](#)]
23. Roberts, M.S.; Magnusson, B.M.; Burczynski, F.J.; Weiss, M. Enterohepatic Circulation: Physiological, pharmacokinetic and clinical implications. *Clin. Pharmacokinet.* **2002**, *41*, 751–790. [[CrossRef](#)] [[PubMed](#)]
24. Hofmann, A.F. The enterohepatic circulation of bile acids in man. *Adv. Intern. Med.* **1976**, *21*, 501–534. [[PubMed](#)]
25. Erlinger, S. Review article: New insights into the mechanisms of hepatic transport and bile secretion. *J. Gastroenterol. Hepatol.* **1996**, *11*, 575–579. [[CrossRef](#)] [[PubMed](#)]
26. Zhang, Z.; Cai, H.X.; Liu, Z.J.; Yao, P. Effective Enhancement of Hypoglycemic Effect of Insulin by Liver-Targeted Nanoparticles Containing Cholic Acid-Modified Chitosan Derivative. *Mol. Pharm.* **2016**, *137*, 2433–2442. [[CrossRef](#)] [[PubMed](#)]
27. Shimada, K.; Mitamura, K.; Higashi, T. Gas chromatography and high-performance liquid chromatography of natural steroids. *J. Chromatog. A* **2001**, *935*, 141–172. [[CrossRef](#)]
28. Tan, J.; Zhou, M.; Cui, X.H.; Wei, Z.C.; Wei, W.X. Discovery of Oxime Ethers as Hepatitis B Virus (HBV) Inhibitors by Docking, Screening and In Vitro Investigation. *Molecules* **2018**, *23*, 637. [[CrossRef](#)]
29. Cui, X.H.; Zhou, M.; Tan, J.; Wei, Z.C.; Wei, W.X.; Luo, P.; Lin, C.W. Design, Synthesis, and Bioactive Screen In Vitro of Cyclohexyl (E)-4-(Hydroxyimino)-4-Phenylbutanoates and Their Ethers for Anti-Hepatitis B Virus Agents. *Molecules* **2019**, *24*, 2063. [[CrossRef](#)]
30. Liu, S.; Wei, W.X.; Li, Y.B.; Liu, X.; Cao, X.; Lei, K.C.; Zhou, M. Design, synthesis, biological evaluation and molecular docking studies of phenylpropanoid derivatives as potent anti-hepatitis B virus agents. *Eur. J. Med. Chem.* **2015**, *95*, 473–482. [[CrossRef](#)]
31. Moiteiro, C.; Marcelo Curto, M.J.; Mohamed, N. Biovalorization of Friedelane Triterpenes Derived from Cork Processing Industry Byproducts. *J. Agric. Food Chem.* **2006**, *54*, 3566–3571. [[CrossRef](#)] [[PubMed](#)]
32. Ramos, S.S.; Almeida, P.; Santos, L. Functionalisation of terpenoids at C-4 via organopalladium dimers: Cyclopropane formation during oxidation of homoallylic σ -organopalladium intermediates with lead tetraacetate. *Tetrahedron* **2007**, *63*, 12608–12615. [[CrossRef](#)]

33. Giorgio, C.; Russo, S.; Incerti, M.; Lodola, A.; Tognolini, M. Biochemical characterization of EphA2 antagonists with improved physico-chemical properties by cell-based assays and surface plasmon resonance analysis. *Biochem. Pharmacol.* **2016**, *99*, 18–30. [[CrossRef](#)] [[PubMed](#)]
34. Cui, J.G.; Huang, L.L.; Huang, Y.M.; Fan, J.C. A Facile Synthesis of a Cholic Acid Derivative with Anticancer Activity. *Chin. J. Org. Chem.* **2009**, *6*, 971–974.
35. Han, Y.Q.; Huang, Z.M.; Yang, X.B.; Liu, H.Z.; Wu, G.X. In vivo and in vitro anti-hepatitis B virus activity of total phenolics from *Oenanthe javanica*. *J. Ethnopharmacol.* **2008**, *118*, 148–153. [[CrossRef](#)]
36. Liu, Y.; Peng, Y.M.; Lu, J.J.; Wang, J.W.; Ma, H.R.; Song, C.J.; Liu, B.J.; Qiao, Y.; Yu, W.Q.; Wu, J.; et al. Design, synthesis, and biological evaluation of new 1, 2, 3-triazolo-2'-deoxy -2'-f luoro-4'-azido nucleoside derivatives as potent anti-HBV agents. *Eur. J. Med. Chem.* **2018**, *143*, 137–149. [[CrossRef](#)]

Sample Availability: Samples of the compounds **01–03** are available from the authors.



© 2020 by the authors. Licensee MDPI, Basel, Switzerland. This article is an open access article distributed under the terms and conditions of the Creative Commons Attribution (CC BY) license (<http://creativecommons.org/licenses/by/4.0/>).